



## INTERNATIONAL JOURNAL OF ENGINEERING SCIENCES & RESEARCH TECHNOLOGY

### Enhancement of Heat Transfer in Solar Air Heater Using Artificial Roughness: A Review

Ankur Vishwakarma <sup>\*1</sup>, Dr. A. R. Jaurker <sup>2</sup>

<sup>\*1</sup> Researcher, Department Of Mechanical Engineering, Jabalpur Engineering College  
Jabalpur, India

<sup>2</sup> Professor, Department Of Mechanical Engineering, Jabalpur Engineering College Jabalpur, India  
[vishwakarma.ankur86@gmail.com](mailto:vishwakarma.ankur86@gmail.com)

#### Abstract

Thermo hydraulic performance of a solar air heater can be improved by enhancing heat transfer between the duct plate and the air. Generally heat transfer enhancement technique categories as Active and Passive technique. Passive technique comprises of adding “Artificial Roughness” that enhances heat transfer by breaking thermal resisting, laminar sub layer. Various roughness geometries with their parameters and correlations are made available by investigators for studying heat transfer enhancement and friction factor. Present paper is a tabulated review of all these geometries, parameters and correlation for suitable selection.

**Keywords:** Artificial Roughness, Heat Transfer, Nusselt Number, Friction Factor.

#### Introduction

Energy plays a vital role in world wide economic and industrial growth. Population growth coupled with material needs escalates its usage a lot. Such rapid increase in energy consumption results in extinguishment of finite energy sources available on earth. Therefore serious attention is to be focused on the alternatives, Solar Energy and Nuclear Energy. Out of the two solar energy shows promising dependence, without the requirement of a highly technical and specialized nature for its wide spread use. The simplest and efficient way to utilize it is to convert it into thermal energy, found application in Solar Air and Water heater. Solar air heater are considered to be compact, less complicated, corrosion and freezing free heaters compare to solar water heaters. The freely available solar radiation provides an infinite and non polluting reservoir of fuel. These are used for heating air that is further utilized for crop drying space heating timber seasoning etc. But thermal efficiency of solar air heaters are low because of low heat transfer capability between absorber plate and the air flowing in the duct. This can be improved by enhancing heat transfer rate. Literature reported that heat transfer can be enhanced by increasing the surface area by using corrugated surface or extended surface called fins. Convective heat coefficient can be increased by creating turbulence at heat transfer surface using artificial roughness. Present paper is an attempt made to categorize and review the reported

roughness geometries used for creating artificial roughness by various investigators. Heat transfer and friction factor correlation developed are also being included.

#### Concept Of Artificial Roughness

The basic cause of thermal resistance between absorber plate and air in solar air heater is presence of laminar sub layer. As the air flows through the duct, a laminar sub layer is formed over the absorber plate that hinders transfer of heat to the flowing air, thereby, adversely affecting thermal performance. Artificially roughened absorber plate is considered to be a good methodology to break laminar sub layer, in order to reduce thermal resistance and increase heat transfer coefficient. The ribs provided by the artificially roughened plate, create local wall turbulence due to flow separation and reattachment between the consecutive ribs, reduce thermal resistance and greatly enhances heat transfer coefficient. Simultaneously an increase in friction factor also being noticed in an artificially roughened duct. It is therefore desirable to create turbulence in near vicinity of heat transferring surface i.e. in laminar sub layer only, in order to reduce friction losses. For selecting the height of roughness element, it is so become imperative to know the thickness of laminar sub layer, which is expressed by the following equation

$$\delta t = 5 \times \frac{v}{ut}$$

**For smooth surface**

$u^+ = y^+$  for laminar sub layer  $y^+ \leq 5$

$u^+ = 5 \ln y^+ + 3.5$  for buffer layer;  $5 \leq y^+ \leq 30$

$u^+ = 2.5 \ln y^+ + 5.5$  for turbulent layer;  $y^+ > 30$

**For roughened surface**

For roughened surfaces, a parameter called roughness Reynolds number ( $e^+$ ) has been defined for flow analysis and is expressed as

$$e^+ = \frac{e}{D} \sqrt{\frac{f}{2}} Re$$

$R(e^+)$  known as momentum transfer function and can be written as

$$R(e^+) = \sqrt{\frac{2}{f}} + 2.5 \ln \frac{2e}{D} + 3.75$$

A similar relation for heat transfer in terms of a heat transfer function  $G(e^+)$  has been developed by Dippery and Sabersky [1] for roughened circular pipes and is expressed as:

$$G(e^+) = \left[ \frac{f}{2\delta t} - 1 \right] \frac{\sqrt{2}}{f} + R(e^+)$$

**Development of correlation and dimensionless variables**

Experimentally data collected by various researchers on various geometries of rib roughened surface has been utilized to develop correlation in following form

$$R(e^+) = R[e^+, p/e, \alpha, \text{duct shape, rib shape}]$$

$$G(e^+) = G[e^+, p/e, \alpha, \text{duct shape, rib shape}]$$

From the above, statistical correlation may be more suitable for design and easy to formulate.

For Nusselt number and friction factor correlation can be expressed as

$$Nu = Nu[Re, e/D, p/e, \alpha, \text{duct shape, rib shape}]$$

$$f = f[Re, e/D, p/e, \alpha, \text{duct shape, rib shape}]$$

**The key dimensionless variables for basic type of roughness geometries are as follows.**

(a) **Shape of roughness element:** The roughness element may be two-dimensional ribs or three dimensional either transverse or inclined of any special form. The common shape of roughness element is Square, circular, semi-circular, chamfered, arc shaped wire, dimple or cavity, compound rib-grooved, and v-shaped continuous or broken ribs with or without gap can be considered to investigate the thermo

hydraulic performance of the solar air heater duct.

(b) **Relative roughness pitch (p/e):** It is the ratio of distance between two consecutive ribs and height of the rib.

(c) **Relative roughness height (e/D):** It is the ratio of rib height to equivalent diameter of the air passage.

(d) **Angle of attack ( $\alpha$ ):** Angle of attack is defined as the inclination of rib with direction of air flow in the duct.

(e) **Aspect ratio:** Aspect ratio is defined as the ratio of duct width to duct height. This factor also plays a very crucial role in investigating thermo-hydraulic performance.

**Effect of rib parameters on flow pattern****Effect of a rib height**

Providing artificial roughness on the underside of the absorber plate creates two flow separation regions, one on each side of the rib, and vortices so generated are responsible for turbulence, which promotes heat transfer accompanied by friction losses. **Fig. 1** shows the effect of rib height on laminar sub layer.

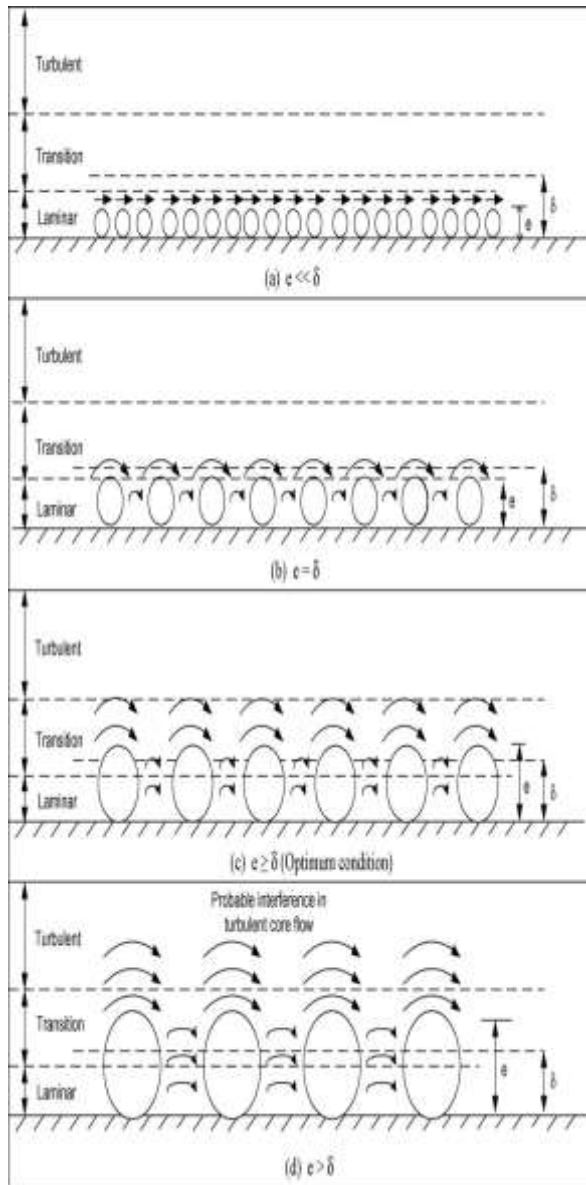


Fig. 1 Effect of rib height on laminar sub layer

**Effect of rib height and pitch**

Figs. 2 and 3 show the flow patterns downstream of a rib with variation in rib height and pitch [1]. The flow separation occurs downstream of a rib and reattachment does not occur if relative roughness pitch ( $p/e$ ) is less than 8. Maximum heat transfer occurs in the vicinity of reattachment point. Similarly, by decreasing the relative roughness pitch ( $p/e$ ) for fixed relative roughness height ( $e/D$ ) or by increasing relative roughness height ( $p/e$ ) for fixed relative roughness height ( $e/D$ ), heat transfer is enhanced. An upper limit of 10 has been imposed on relative roughness pitch ( $p/e$ ) beyond which there is a decrease in heat transfer enhancement.

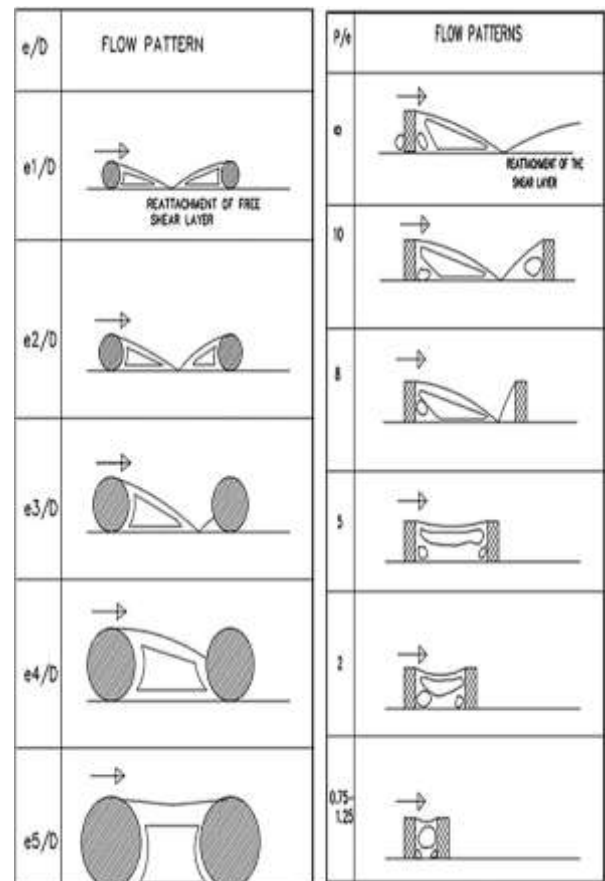


Fig. 2. Effect of rib roughness height ( $e_5 > e_4 > e_3 > e_2 > e_1$ ,  $p = \text{constant}$ ).

Fig. 3. Flow pattern of rib as a function of relative roughness pitch.

**Effect of width and position of gap in continuous inclined rib**

With the introduction of a gap in a rib, secondary flow along the rib joins the main flow to accelerate it, which in turn, energizes the retarded boundary layer flow along the surface resulting in enhancement of heat transfer. Position of gap with respect to leading and trailing edge has a considerable effect on heat transfer enhancement. Position of the gap near the trailing edge, results in more contribution of secondary flow in energizing the main flow through the gap and recirculation loop in the remaining part of the rib, thereby, increasing the heat transfer rate.

**Effect of V-shaping of rib**

Shaping of a long, angled rib into v-shape helps in the formation of two leading ends (where heat transfer rate is high) and a single trailing end (where heat transfer is low) resulting in much large area of heat transfer. V-shaped ribs form two secondary flow cells as compared to one in case of a straight angled rib resulting in higher overall heat

transfer coefficient in case of v-shaped rib as shown in Fig. 4. V-shaped rib with apex facing downstream has a higher heat transfer as compared to that of with apex facing upstream.

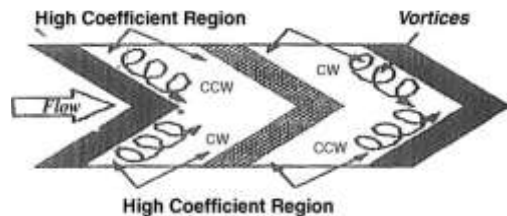


Fig. 4. Effect of V-shaping of rib.

**Effect of discretizing of V-shaped ribs**

The V-shaped ribs along with staggered rib pieces in between further increase the number and area of heat transfer regions. Additional rib parameters related to the size and positioning of rib pieces (length ratio, B/S, segment ratio, S/S and staggering ratio, P/P) with respect to main rib produce complex interaction of secondary flow.

**Effect of rib cross-section**

Rib cross-section affects the size of separated region and level of disturbance in the flow. The friction factor is less for circular cross-section ribs in comparison to that of rectangular or square cross-section ribs on account of reduction in the size of separated region. This results in decrease in inertial losses and increase in skin friction, thereby, decreasing the friction factor. As the size of separated region diminishes, level of disturbance in flow also decreases which affects the heat transfer adversely. Another possible factor contributing to the Nusselt number decrease is the reduction in heat transfer surface area associated with circular cross-section ribs.

**Roughness geometries used in solar air heaters**

About 147 year ago, attempt to enhance heat transfer coefficients in condensing steam was reported in the classical study by **JP Joule [2]**.

The use of artificial roughness in solar air heaters owes its origin to several investigations carried out in connection with the enhancement of heat transfer in nuclear reactors, cooling of turbine blades and electronic equipment. Important roughness geometries reported in literature are shown in Figs. 5 [3-4].

The general arrangement of different types of roughness geometries reported by the various Investigators can be divided in four categories.

- Wire Fixation
  - Transverse continuous ribs
  - Transverse broken ribs

Inclined and V-shaped or staggered ribs

- Rib formation by Machining process
  - Chamfered ribs
  - Wedge shaped ribs
  - Combination of different integral rib roughness elements
- Wire mesh or Expanded metal mesh ribs
- Dimple/protrusion shaped geometry

**Kays [5] [1966]**, suggested the use of small diameter circular wires to artificially roughen the heat transferring surface of a heat exchanger to enhance heat transfer and recommended that in order to make the use of artificial roughness more effective, the height of roughness element should be kept small, primarily in the sub layer region, so that the increases in the friction will not be disproportionate to the increase in heat transfer.

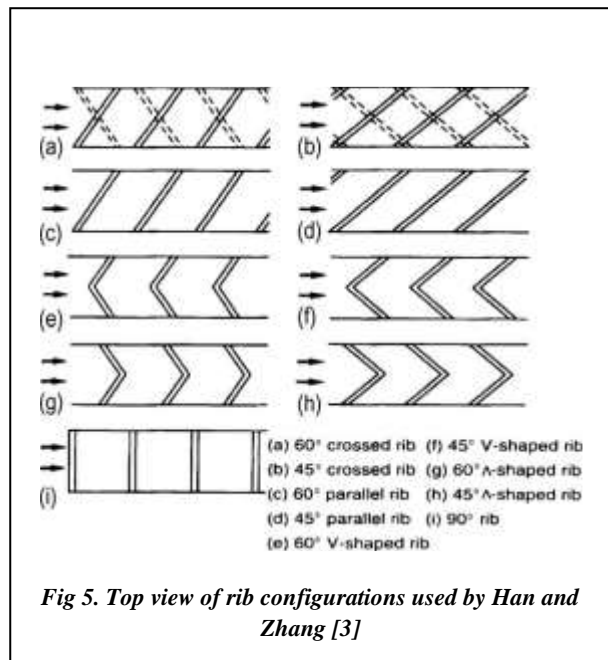


Fig 5. Top view of rib configurations used by Han and Zhang [3]

compared the Nusselt number, friction factor and plate efficiency factor of roughened corrugated and plane absorber plates with that of plane corrugated and smooth absorber plates. The protruding wires enhanced the heat transfer coefficient for the roughened air heaters and plate efficiency factor improved from 0.63 to 0.72 resulting in 14% improvement in the performance.

**Prasad and Saini [7, 8] [1998]**, studied the effect of roughness and flow parameters such as relative roughness height (e/D) and relative roughness pitch (p/e) on heat transfer and friction factor. The type and orientation of roughness geometry used have been shown in Fig. 6. They developed expressions for the heat transfer and friction factor for a fully



turbulent flow. It was observed that maximum heat transfer occurred in the vicinity of reattachment points and reattachment of free shear layer does not occur if relative roughness pitch ( $p/e$ ) is less than about 8 to 10. Optimal thermo hydraulic performance is achieved for roughness height slightly higher than the transition sub layer thickness. For relative roughness height ( $e/D$ ) value of 0.033 and relative roughness pitch ( $p/e$ ) value of 10, maximum enhancement in Nusselt number and friction factor was reported to be 2.38 and 4.25 times respectively over smooth duct.

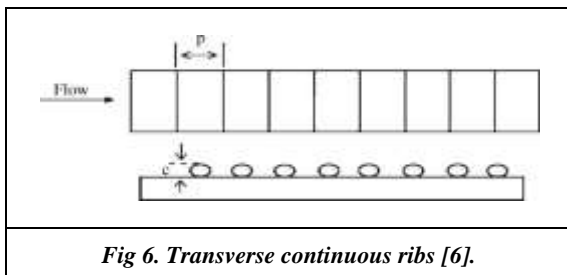


Fig 6. Transverse continuous ribs [6].

Verma and Prasad [9], conducted an outdoor experimental investigating the thermo hydraulic optimization of the roughness and flow parameters for Reynolds number ( $Re$ ) range of 5000–20,000, relative roughness pitch ( $p/e$ ) range of 10–40 and relative roughness height ( $e/D$ ) range of 0.01–0.03. The optimal value of roughness Reynolds number ( $e+$ ) was found to be 24 and corresponding to this value, optimal thermo hydraulic performance was reported to be 71%. Heat transfer enhancement factor was found to vary between 1.25 and 2.08 for the range of parameters investigated.

#### Transverse broken ribs with circular cross-section

Sahu and Bhagoria [10] [2005], investigated the effect of  $90^\circ$  broken ribs on thermal performance of a solar air heater for fixed roughness height ( $e$ ) value of 1.5 mm, duct aspect ratio ( $W/H$ ) value of 8, pitch ( $p$ ) in the range of 10–30 mm and Reynolds number ( $Re$ ) range of 3000–12,000. Roughened absorber plate increased the heat transfer coefficient by 1.25 to 1.4 times as compared to smooth one under similar operating conditions. Corresponding to roughness pitch ( $p$ ) value of 20 mm, maximum value of Nusselt number was obtained that decreased on the either side of this roughness pitch ( $p$ ) value. Based on the experimental investigation, the thermal efficiency of roughened solar air heater was found to be in the range of 51–83.5% depending upon the flow conditions. The geometry investigated has been shown in Fig.7.

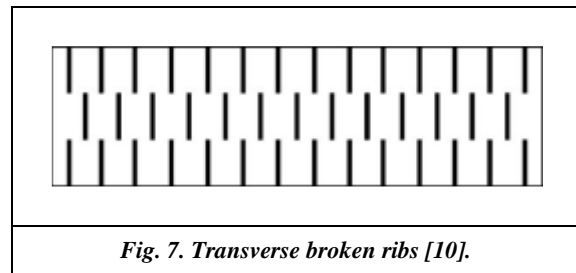


Fig. 7. Transverse broken ribs [10].

#### Inclined continuous ribs

Gupta et al. [11] [1993], experimentally investigated the effect of relative roughness height ( $e/d$ ), inclination of rib with respect to flow direction and Reynolds number ( $Re$ ) on the thermo hydraulic performance of a roughened solar air heater for transitionally rough flow region ( $5 < e+ < 70$ ). The roughness geometry investigated has been shown in Fig.8. It was reported that with increase in relative roughness height ( $e/d$ ), the value of Reynolds number ( $Re$ ) decreased for which effective efficiency was maximum. The effective efficiency also increased with increase in insolation. For a roughened solar air heater, maximum enhancement in heat transfer and friction factor was reported to be of the order 1.8 and 2.7 times respectively corresponding to angle of inclination values of  $60^\circ$  and  $70^\circ$ , respectively. The best thermo hydraulic performance was reported for relative roughness height ( $e/D$ ) value of 0.023 and Reynolds number ( $Re$ ) value of 14,000.

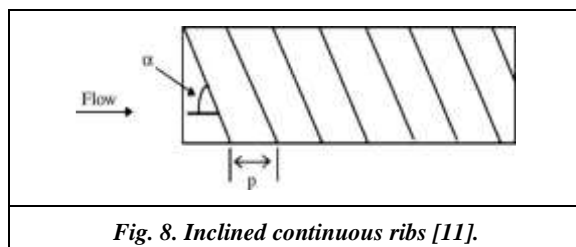


Fig. 8. Inclined continuous ribs [11].

Aharwal et al. [12] [2008], experimentally studied the effect of width and position of gap in inclined split-ribs having square cross-section on heat transfer and friction characteristics of a rectangular duct. The duct had an aspect ratio ( $W/H$ ) of 5.84, relative roughness pitch ( $p/e$ ) of 10, relative roughness height ( $e/D$ ) of 0.0377, angle of attack ( $\alpha$ ) of  $60^\circ$ , relative gap width ( $g/e$ ) range of 0.5–2 and relative gap position ( $d/W$ ) varied from 0.1667 to 0.667 for Reynolds number ( $Re$ ) range of 3000–18,000. For the split-rib and continuous rib roughened ducts, the enhancement in heat transfer was reported to be in the range of 1.71–2.59 and 1.48–2.26 times respectively over smooth duct under similar operating conditions. The maximum values of heat transfer, friction factor ratio ( $f/fs$ ) and thermo hydraulic parameter so obtained were corresponding to relative gap width ( $g/e$ ) value of

1.0 and relative gap position ( $d/W$ ) value of 0.25 for the range of parameters investigated. Particle Image Velocimetry (PIV) system was used to visualize the effects of angle of inclination of ribs on the flow behavior. Based on experimental results, correlations for Nusselt number and friction factor were developed.

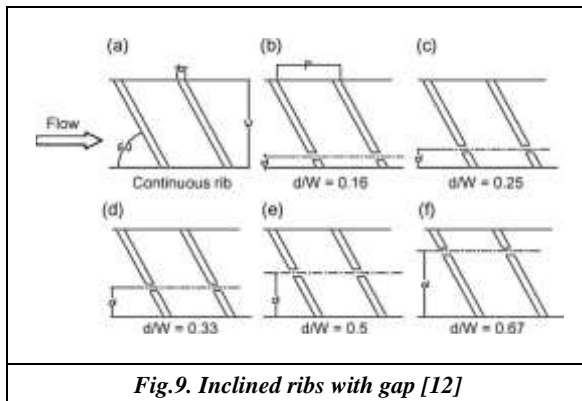


Fig.9. Inclined ribs with gap [12]

#### V-shaped ribs

Momin et al. [13], experimentally investigated the effect of geometrical parameters of v-shaped ribs, shown in Fig. 10, on heat transfer and fluid flow characteristics of rectangular duct of a solar air heater. The investigation covered a Reynolds number ( $Re$ ) range of 2500–18,000, relative roughness height ( $e/D$ ) range of 0.02–0.034 and angle of attack of flow ( $\alpha$ ) range of 30–90° for a fixed relative roughness pitch ( $p/e$ ) value of 10. Rate of increase of Nusselt number was observed to be lower than the rate of increase of friction factor with an increase in Reynolds number ( $Re$ ). The maximum enhancement of Nusselt number and friction factor as result of providing artificial roughness had been found to be 2.30 and 2.83 times respectively over the smooth duct for an angle of attack ( $\alpha$ ) of 60°. It was reported that for relative roughness height ( $e/D$ ) value of 0.034 and angle of attack ( $\alpha$ ) of 60°, v-shaped ribs enhanced the value of Nusselt number by 1.14 and 2.30 times over inclined ribs and smooth absorber plate respectively. Correlations for Nusselt number and friction factor were developed.

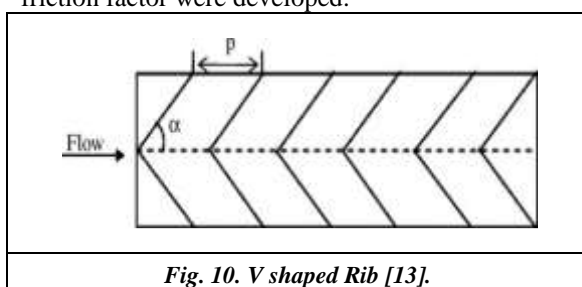


Fig. 10. V shaped Rib [13].

Muluwork et al. [14] compared the thermal performance of staggered discrete v-apex up and

down ribs with corresponding transverse staggered discrete ribs shown in Fig. 11. They studied the effect of relative roughness length ratio ( $B/S$ ), relative roughness segment ratio ( $S'/S$ ), relative roughness staggering ratio ( $p'/p$ ) and angle of attack ( $\alpha$ ) on the heat transfer and friction factor. It was observed that the Nusselt number increased with the increase in relative roughness length ratio ( $B/S$ ). Nusselt number for v-down discrete ribs was found to be higher than the corresponding v-up and transverse discrete roughened surfaces. Nusselt number increased with increase in relative roughness staggering ratio ( $p'/p$ ) and attained a maximum value for relative roughness staggering ratio ( $p'/p$ ) value of 0.6. Heat transfer and friction factor attained maximum values for angle of attack (a) 60° and 70°, respectively. Correlations for Nusselt number and friction factor were developed.

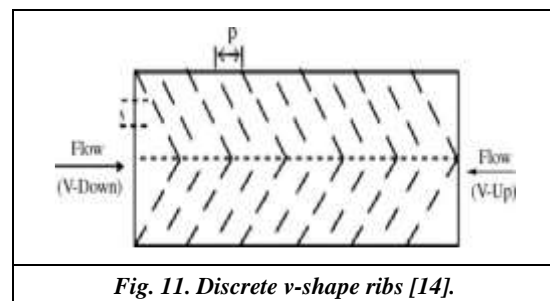


Fig. 11. Discrete v-shape ribs [14].

Sukhmeet Singh, Subhash Chander, J.S. Saini [15], studied the heat and fluid flow characteristics of rectangular duct having its one broad wall heated and roughened with periodic 'discrete V-down rib' are experimentally investigated. Reynolds number ( $Re$ ) has been varied from 3000–15000 with relative gap width ( $g/e$ ) and relative gap position ( $d/w$ ) range of 0.5–2.0 and 0.20–0.80 respectively. The respective variation in relative roughness pitch ( $P/e$ ), angle of attack ( $\alpha$ ) and relative roughness height ( $e/D_h$ ) have been 4–12, 30–75 and 0.015–0.043. The effect of roughness parameters on Nusselt number ( $Nu$ ) and friction factor ( $f$ ) has been determined and the results obtained were compared with those of smooth duct. The maximum increase in  $Nu$  and  $f$  over that of smooth duct was 3.04 and 3.11 folds respectively.

#### Multiple V-ribs

V.S. Hans, R.P. Saini, J.S. Saini [2010] [16], The experiment encompassed Reynolds number ( $Re$ ) from 2000 to 20000, relative roughness height ( $e/D$ ) values of 0.019–0.043, relative roughness pitch ( $P/e$ ) range of 6–12, angle of attack ( $\alpha$ ) range of 30–75 and relative roughness width ( $W/w$ ) range of 1–10. Extensive experimentation has been conducted to collect data on heat transfer and fluid flow characteristics of a rectangular duct roughened with multiple v-ribs. A maximum

enhancement of Nusselt number and friction factor due to presence of such an artificial roughness has been found to be 6 and 5 times, respectively, in comparison to the smooth duct for the range of parameters considered.

**Karwa [17]**, carried out a comparative experimental study of augmented heat transfer and friction in a rectangular duct with rectangular cross-section ribs arranged in V-continuous and V discrete pattern for duct aspect ratio (W/H) range of 7.19–7.75, relative roughness pitch (p/e) value 10, relative roughness height (e/D) range of 0.0467–0.050 and Reynolds number (Re) range of 2800–15,000. The enhancement in the Stanton number over the smooth duct was reported to be in range of 102–137%, 110–147%, 93–134% and 102–142% for transverse inclined, V-up continuous, V-down continuous, v-up discrete and V-down discrete rib arrangement, respectively. The friction factor ratios corresponding to these arrangements were found as 3.02–3.42, 3.40–3.92, 3.32–3.65, 2.35–2.47 and 2.46–2.58, respectively. The performance of V-down ribs was observed to be better than that of V-up ribs, which was in confirmation with the findings of **Muluwork et al. [14]**. The rib configurations investigated in the study have been shown in **Fig. 12**.

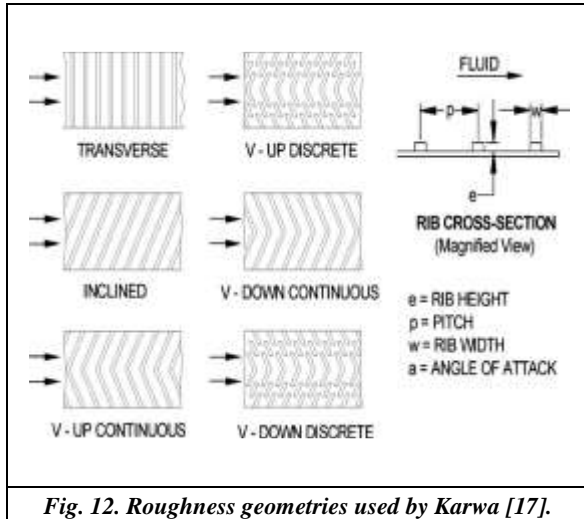


**Fig. 12. Roughness geometries used by Karwa [17].**

**Arc shaped ribs**

**Saini and Saini [19]**, studied the effect of arc shaped ribs on the heat transfer coefficient and friction factor of rectangular ducts with Reynolds number (Re), relative roughness height (e/D) and relative arc angle (a) varying from 2000 to 17,000, 0.0213 to 0.0422 and 0.3333 to 0.6666, respectively. It was reported that relative arc angle (a) had an opposite effect on heat transfer enhancement and friction factor. With decrease in

relative arc angle (a) value, Nusselt number value increased while friction factor value decreased. Enhancement of Nusselt number and friction factor was reported to be of order 3.6 and 1.75 times respectively over smooth duct for relative arc angle (a) value of 0.3333 and relative roughness height (e/D) value of 0.0422. Based on the experimental results, correlations for Nusselt number and friction factor were developed. The geometry investigated has been shown in **Fig. 13**.

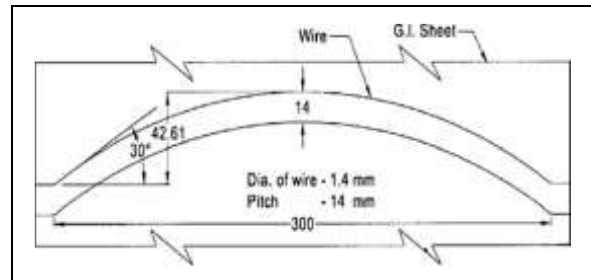


**Fig. 13. Arc shape ribs [19].**

**Karmare and tikekar [20] [2007]** Experimentally investigated the effect on heat transfer coefficient and friction factor by providing the metal ribs of the circular cross section in a staggered manner on absorber plate in solar air heater as depicted in fig.7. The highest heat transfer rate was found for  $l/s=1.72$ ,  $e/D=0.044$  and  $p/e =17.5$ , were the highest friction factor was found for  $l/s=1.72$ ,  $e/D=0.044$  and  $p/e =12.5$ . Enhancement in the Nusselt number was found to be 187% and friction factor by 213% as compared with the smooth plate. Optimum performance was observed for  $l/s=1.72$ ,  $e/D=0.044$  and  $p/e =17.5$ .

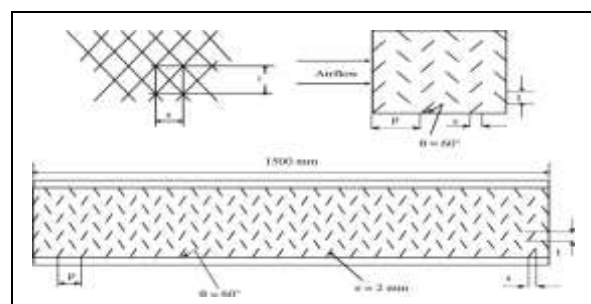


**Fig.14. Metal grit ribs [20].**

**Kumar et al. [21] [2008]** carried out an experimental investigation to determine the heat transfer distributions in solar air heater having its absorber plate roughened with discrete w-shaped ribs. The experiment encompassed Reynolds number (Re) range from 3000 to 15,000, rib height (e) values of 0.75 mm and 1 mm, relative roughness height (e/D) 0.0168 and 0.0225 and relative roughness pitch (p/e) of 10 and angle of

attack (a) 458. Thermal performance of roughened solar air collector was compared with that of smooth one under similar flow conditions and it was reported that thermal performance of the roughened channel was 1.2–1.8 times the smooth channel for range of parameters investigated. Discretization was found to have significant effect on heat transfer enhancement. The geometry investigated has been shown in Fig. 13.

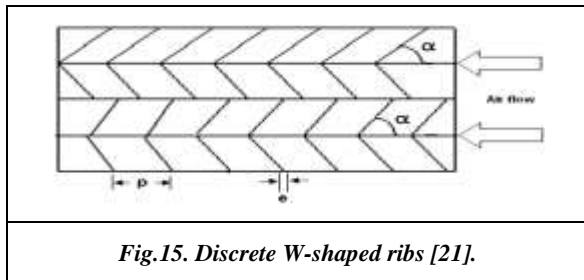


Fig.15. Discrete W-shaped ribs [21].

**RIB FORMATION BY MACHINING PROCESS**

*Chamfered ribs*

**Rajendra Karwa, S.C. Solanki, J.S. Saini [23].** Investigation of the performance of solar air heaters with chamfered repeated rib-roughness on the airflow side of the absorber plates as shown in Fig.16. The roughened elements have a relative roughness pitch of 4.58 and 7.09 while the rib chamfer angle is fixed at 15°. For the airflow duct depths of 21.8, 21.5 and 16 mm, the relative roughness heights for the three roughened plates used are 0.0197, 0.0256 and 0.0441, respectively. The airflow rate per unit area of absorber plate has been varied between 0.024 to 0.102 kgs/m<sup>2</sup> (flow Reynolds number ranges from 3750 to 16350). The study shows substantial enhancement in thermal efficiency (10 to 40%) over solar air heaters with smooth absorber plates due to the enhancement in the Nusselt number (50% to 120%).

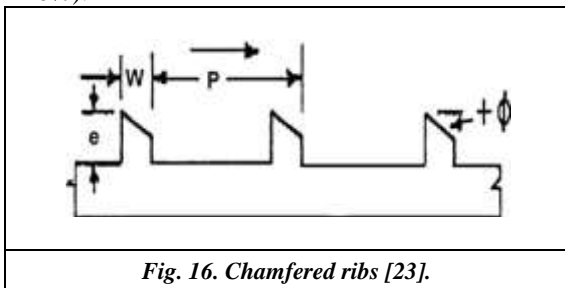


Fig. 16. Chamfered ribs [23].

*Wedge shaped ribs*

**J.L. Bhagoria et al. [24],** experimentally studied heat transfer and flow characteristics in a solar air heater having absorber plate roughened with wedge shaped transverse integral ribs as shown in Fig. 17.

The investigation encompassed the Reynolds number (Re) range of 3000–18,000, relative roughness height (e/D) range of 0.015–0.033 and rib wedge angle (F) range of 8–128. It was reported that Nusselt number and friction factor increased by 2.4 and 5.3 times over smooth duct in the range of parameters investigated. Statistical correlations for Nusselt number and friction factor were developed.

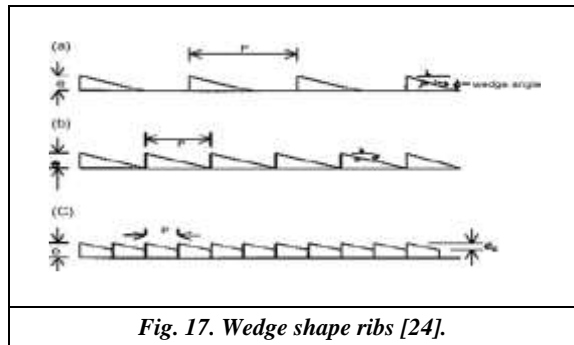


Fig. 17. Wedge shape ribs [24].

*Combination of inclined and transverse ribs*

**A.R. Jaurker, J.S. Saini, B.K. Gandhi et al. [25],** experimentally investigated heat transfer and friction characteristics of rib-groove roughened rectangular duct as shown in Fig. 18. The experimental investigation encompassed the Reynolds number range from 3000 to 21,000; relative roughness height 0.0181–0.0363, relative roughness pitch 4.5–10.0 and groove position to pitch ratio 0.3–0.7. As compared to the smooth duct, the presence of rib grooved artificial roughness yields Nusselt number rises up to 2.7 times while the friction factor rises up to 3.6 times in the range of parameters investigated. The optimum condition for heat transfer occurs at a groove position to pitch ratio of 0.4, while on the either side of this ratio, both Nusselt number and friction factor decreases.

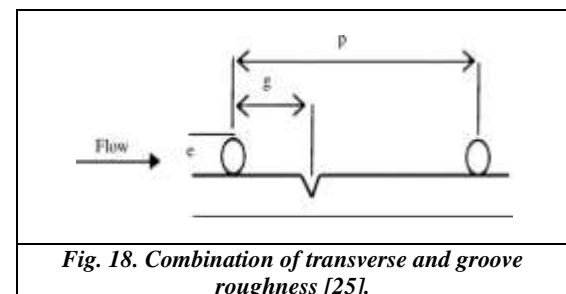
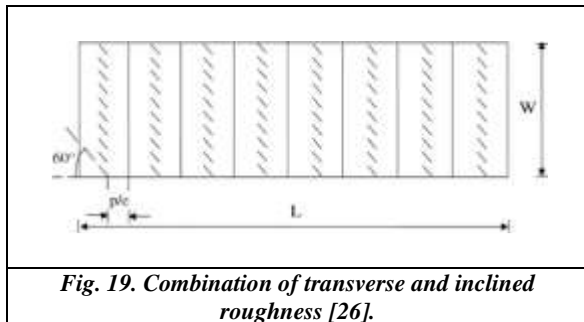


Fig. 18. Combination of transverse and groove roughness [25].

**Varuna, R.P. Sainib, S.K. Singal [26],** carried out an experimental study on heat transfer and friction characteristics by using a combination of inclined and transverse ribs on the absorber plate of a solar air heater with Reynolds number (Re) ranging from



2000 to 14,000, relative roughness pitch ( $p/e$ ) range of 3–8, relative roughness height ( $e/D$ ) value of 0.030, duct aspect ratio ( $W/H$ ) value of 10 and roughness height ( $e$ ) value of 1.6 mm. For relative roughness pitch ( $p/e$ ) value of 8, the best thermal performance was reported. Correlations for Nusselt number and friction factor were developed. The geometry investigated has been shown in **Fig. 19**



**Fig. 19. Combination of transverse and inclined roughness [26].**

**Expanded Metal Mesh**

**Saini and Saini [27] [1997]**, carried out an experimental investigation to study the effect of wire mesh roughened absorber plate on heat transfer augmentation and friction characteristics of solar air heater as shown in **Fig. 20**. The investigation considered relative long way length of mesh ( $L/e$ ) in range of 25–71.87, relative short way length of mesh ( $S/e$ ) in range of 15.62–46.87, relative roughness height ( $e/D$ ) in range of 0.12–0.039 and Reynolds number ( $Re$ ) in range of 1900–13,000. It was reported that the maximum heat transfer of order 4 times over the smooth duct was obtained corresponding to angle of attack of 61.98; relative long way length of mesh ( $L/e$ ) value of 46.87 and relative short way length of mesh ( $S/e$ ) value of 25. Maximum value of friction factor was reported for angle of attack of 72°, relative long way length of mesh ( $L/e$ ) value of 71.87 and relative short way length of mesh ( $S/e$ ) value of 15. Correlations for Nusselt number and friction factor were developed.

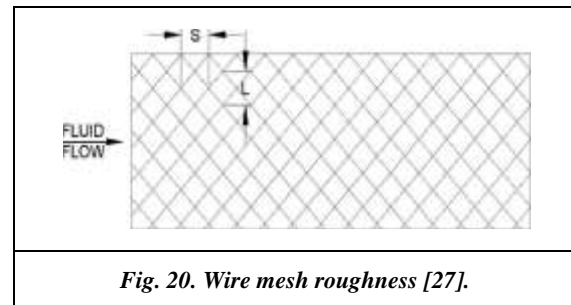


**Fig. 20. Wire mesh roughness [27].**

**Dimpled Surfaces**

**Saini and Verma [28]**, studied the effect of roughness and operating parameters on heat transfer and friction factor in a roughened duct provided with dimple-shape roughness geometry for the range of Reynolds number ( $Re$ ) from 2000 to 12,000, relative roughness height ( $e/D$ ) from 0.018 to 0.037 and relative pitch ( $p/e$ ) from 8 to 12. For the range of parameters investigated, Nusselt number was found to be maximum corresponding to relative roughness height ( $e/D$ ) value of 0.0379 and relative roughness pitch ( $p/e$ ) value of 10. For fixed value of relative roughness pitch ( $p/e$ ) of 10, friction factor attained the maximum and minimum values corresponding to relative roughness height ( $e/d$ ) values of 0.0289 and 0.0189, respectively. Correlations for Nusselt number and friction factor have been developed. The geometry investigated has been shown in **Fig. 21**.

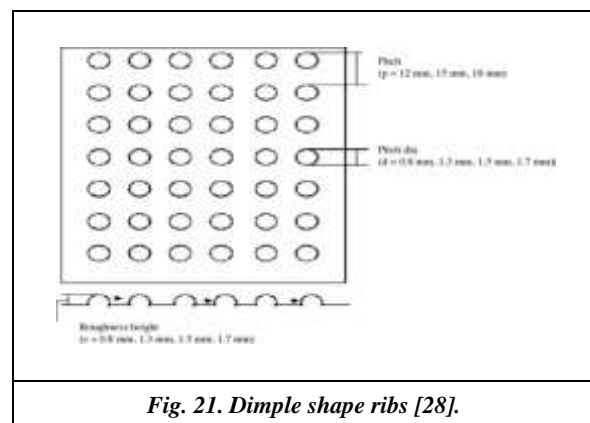


**Fig. 21. Dimple shape ribs [28].**

**Table 1: Correlations developed for heat transfer and friction factor for different roughness geometries used in solar air heaters.**

Author	Parameters	Heat transfer	Friction factor
Prasad and Saini	(e/D):0.020-0.033	$St = \frac{f/2}{1 + \sqrt{f}/2\{4.5(e+)^{0.28} Pr^{0.57} 0.957(P/e)^{0.55}\}}$	$f = \frac{(W + 2B)fs + Wfs}{2(W + B)}$ $fr = \frac{2}{[0.95(P/e)^{0.53} + 2.5 \ln\left(\frac{D}{2e}\right) - 3.75]^2}$
Aharwal et al.	(P/e):10-20 Re:5000-50000 (e/D):0.0377	$Nu = 0.002Re^{1.08} (e/D)^{1.87}$ $\times \exp[-0.45\text{Ln}(P/e)^2](\alpha/60)^{0.006}$ $\times \exp[-0.65\text{Ln}(\alpha/60)^2](d/W) - 0.32$ $\times \exp[-0.12\text{Ln}(d/W)^2](g/e) - 0.03$ $\times \exp[-0.18\text{Ln}(g/e)^2](e/D)^{0.5}$	$f = 0.071Re - 0.133(P/e)^{1.83}$ $\times \exp[-0.44\text{Ln}(P/e)^2](d/W)$ $- 0.43$ $\times \exp[-0.14\text{Ln}(d/W)^2](g/e)$ $- 0.052 \times (\alpha/60)^{0.67}$ $\times \exp[-0.12\text{Ln}(g/e)^2](e/D)^{0.69}$
Muluwork and Saini	g/e:0.5-2 d/w: 0.1667-0.667 W/H:5.84 $\alpha : 60^\circ$ Re: 3000-18000 e/D:0.01-0.05	$Nu = 0.00534Re^{1.299}(B/S)^{1.346}(S'/S)^{1.112}(e/D)^{0.270}(P'/P)^{0.762} \exp[-2.25(\text{Ln}(P'/P)^2)] [-0.376\text{Ln}(1 - \alpha/60)]$	$f = 0.7117Re^{-0.299} \left(\frac{B}{S}\right)^{0.636} (S'S)^{0.712}(D)^{0.113} (P'/P)^{-0.0936} \exp[-1.26(\text{Ln}(1 - \alpha/70))^2]$

Verma and Prasad	P'/P:0.2-0.8 S'/S:1.1-2.3 B/S:3-9 $\alpha$ : 60-90 Re:3032-17652 e/D:0.02-0.034	$Nu = 0.08596 \left(\frac{P}{e}\right)^{-0.054} (e/D)^{0.0722} Re^{0.723} \text{ for } e+ \leq 24$ $Nu = 0.02954 \left(\frac{P}{e}\right)^{-0.016} (e/D)^{0.021} Re^{0.802} \text{ for } e+ > 24$	$f = 0.245 \left(\frac{P}{e}\right)^{-0.206} (e/D)^{0.243} Re^{-1.25}$
Gupta	(P/e):10-40 Re: 5000-20000 (e/D): 0.020-0.05 $\alpha$ : 30 <sup>0</sup> -90 <sup>0</sup>	$Nu = 0.0024 \left(\frac{e}{D}\right)^{0.001} (W/H)^{-0.06} Re^{1.084} \times \exp\left[-0.004 \left(1 - \frac{\alpha}{60}\right)^2\right] \text{ for } e+ < 35$ $Nu = 0.0071 \left(\frac{e}{D}\right)^{-0.24} (W/H)^{-0.028} Re^{0.88} \times \exp\left[-0.475 \left(1 - \frac{\alpha}{60}\right)^2\right] \text{ for } e+ \geq 35$	$f = 0.1911 \left(\frac{e}{D}\right)^{0.196} \left(\frac{W}{H}\right)^{-0.093} (Re)^{1.084} \times \exp[-0.993(1 - \alpha/70)^2]$
Saini & Saini	(e/D): 0.012-0.039 (S/e):15062-42.87 (L/e):25-71.87 (Re):1900-13000	$Nu = 4.0 \times 10^{-4} \times Re^{1.22} \left(\frac{e}{D}\right)^{0.625} (S/e)^{2.22} \times \exp\left[-1.25 \left\{Ln\left(\frac{S}{10e}\right)\right\}^2\right] (L/e)^{2.26} \times \exp\left[-0.824 \left\{Ln\left(\frac{L}{10e}\right)\right\}^2\right]$	$f = 0.815 Re^{0.361} \left(\frac{L}{e}\right)^{0.266} \left(\frac{S}{10e}\right)^{-0.19} (10(e/D))^{0.591}$
Momin	(e/d):0.01-0.03 (P/e):10-40 Re:2500-18000	$Nu = 0.067 Re^{0.888} \left(\frac{e}{D}\right)^{0.424} (\alpha/60)^{-0.077} \exp[-0.782(Ln(\alpha/60))^2]$	$f = 6.266 Re^{-0.425} \left(\frac{e}{D}\right)^{0.565} (\alpha/60)^{-0.093} \exp[-0.719 \times (Ln \alpha/60)^2]$

<p>Karwa</p>	<p>(W/H):4.8,6.1,7.8,9                  .66 and 12                  (e/D):0.0141-                  0.0328                  (P/e): 4.5,5.8,7 and                  8.5                  ϕ: 15-18                  Re:3000-20000</p>	$g = 103.77e^{-0.006\phi} \left(\frac{W}{H}\right)^{0.5} (P/e)^{-2.56}$ $\times \exp\left[0.7343 \left\{\ln\left(\frac{P}{e}\right)\right\}^2\right] (e+)^{-0.31}$ $g = 32.26 \left(\frac{W}{H}\right)^{0.5} (P/e)^{-2.56}$ $\times \exp\left[0.7433 \left\{\ln\left(\frac{P}{e}\right)\right\}^2\right] (e+)^{-0.08}$	$R = 1.66e^{-0.0078\phi} \left(\frac{W}{H}\right)^{-0.4} (P/e)^{2.695} \times$ $\exp\left[-0.762 \left\{\ln\left(\frac{P}{e}\right)\right\}^2\right] (e+)^{-0.075} \text{ for } 5 \leq e+ < 20$ $R = 1.325e^{-0.0078\phi} \left(\frac{W}{H}\right)^{-0.4} (P/e)^{2.695} \times$ $\exp\left[-0.762 \left\{\ln\left(\frac{P}{e}\right)\right\}^2\right] \text{ for } 20 \leq e+ < 60$
<p>Bhagoria et al.</p>	<p>(e/d):0.015-0.033                  (P/e):60.17  <math>\phi^{-1.0264} &lt; (P/e) &lt; 12</math>.                  15.2013                  Re:3000-18000</p>	$Nu = 1.89 \times 10^{-4} Re^{1.21} \left(\frac{e}{d}\right)^{0.426} (P/e)^{2.94}$ $\times \exp\left[-0.71 \left\{\ln\left(\frac{P}{e}\right)\right\}^2 \left(\frac{\phi}{10}\right)\right]$ $\times \exp[-1.5\{\ln(\phi/10)\}]$	$f = 12.44Re^{-0.18} ((e/d)^{0.99}) \left(\frac{P}{e}\right)^{-0.52} ((\phi/10)^{0.49})$



Saini and Saini	(P/e):10 (e/d):0.021-0.042 Re:2000-17000 (α/90):0.33-0.66	$Nu = 0.001047 Re^{1.3186} \left(\frac{e}{d}\right)^{0.3772} \times (\alpha/90)^{-0.1198}$	$f = 0.14408 Re^{-0.17103} ((e/d)^{0.1765}) ((\phi/10)^{0.1185})$
Saini and Verma	(P/e):8-10 (e/d):0.018-0.037 Re:2000-12000	$Nu = 5.2 \times 10^{-4} Re^{1.27} (P/e)^{3.15} \times \exp\left[-2.21 \left\{\ln\left(\frac{P}{e}\right)\right\}^2\right] (e/D)^{0.033} \times [\exp(-1.3)\{\ln(e/D)\}^2]$	$f = 0.642 Re^{-0.423} \left(\frac{P}{e}\right)^{-0.465} \left[\exp(0.054) \left(\log\left(\frac{P}{e}\right)\right)^2\right] \times (e/D)^{-0.0214} [\exp(0.84)(\log(e/d)^2)]$
Karmare & tikekar	(e/D):0.035-0.044 (P/e):12.5-36 (Re):4000-17000	$Nu = 2.4 \times 10^{-4} Re^{1.3} \times \left(\frac{e}{D}\right)^{0.42} \left(\frac{l}{s}\right)^{-0.146} (P/e)^{-0.27}$	$f = 15.55 \times Re^{-0.263} \times \left(\frac{e}{d}\right)^{0.91} \left(\frac{l}{s}\right)^{-0.27} (P/e)^{-0.51}$

## Conclusion

Thermal efficiency of solar air heater can be increased by enhancing heat transfer between the absorber plate and the air flowing in the duct. Thus increasing the contact area between air and absorber plate is essential. Investigator achieved this by providing artificial roughness on the underside of the absorber plate. Various roughness geometries provided shows comparable result in the improvement of heat transfer, for solar air heater. Friction offered to air flow by these roughness geometries, accounted as friction factor, act as a penalty with enhancement of thermal performance of solar air heater using roughened duct.

- Roughened duct shows appreciable increase in heat transfer as compare to smooth duct.
- Different roughness geometries provided on the plate shows different heat transfer rate when compared to each other as well as to smooth plate.
- Flow of air in relation to roughness geometry shows variable rate of heat transfer
- Ex. V shaped rib pointing downstream gives better heat transfer as compare to V shaped rib pointing upstream.
- Angle of attack of air  $\alpha = 45^\circ$  &  $30^\circ$  shows the best thermal performance with parallel full rib.
- Heat transfer in a rectangular duct with a dimple surface gives 2.1 times heat transfer enhancement, regardless of the channel height.
- Friction factor also improves as a by – product, adding penalty to solar air heater performance.

### Nomenclature

$A_c$  surface area of absorber plate,  $m^2$   
 $B$  half-length of full V-rib element, m  
 $C_p$  specific heat of air, J/kg K  
 $D$  equivalent diameter of duct, m  
 $D_h$  hydraulic diameter of duct, m  
 $d$  parameter of broken rib, m,  
 $e$  rib height, m  
 $g$  groove position, m  
 $h$  heat transfer coefficient,  $W/m^2 K$   
 $H$  depth of air duct, m  
 $I$  intensity of solar radiation,  $W/m^2$   
 $K$  thermal conductivity of air,  $W/mK$   
 $L$  length of test section of duct or long way length of mesh, m  
 $m$  mass flow rate, kg/s  
 $P$  pitch, m  
 $D_p$  pressure drop, Pa  
 $q_u$  useful heat flux,  $W/m^2$   
 $Q_u$  useful heat gain, W  
 $Q_l$  heat loss from collector, W  
 $Q_t$  heat loss from top of collector, W  
 $S$  length of discrete rib or short way length of mesh, m  
 $T_o$  fluid outlet temperature, K  
 $T_i$  fluid inlet temperature, K  
 $T_a$  ambient temperature, K  
 $T_{pm}$  mean plate temperature, K  
 $T_{pm}$  mean air temperature, K  
 $U_L$  overall heat loss coefficient,  $W/m^2$   
 $v$  velocity of air in the duct, m/s  
 $w$  width of rib, m  
 $W$  width of duct, m

### Dimensionless parameters

$B/S$  relative roughness length  
 $d/W$  relative gap position

$e^+$  roughness Reynolds number  
 $e/D_h$  relative roughness height  
 $e/H$  rib to channel height ratio  
 $f$  friction factor  
 $f_r$  average friction factor  
 $F_R$  heat removal factor  
 $g/e$  relative gap width  
 $g/P$  relative groove position  
 $G$  momentum heat transfer function  
 $L/e$  relative long way length of mesh  
 $l/s$  relative length of metal grit  
 $Nu$  Nusselt number  
 $\bar{N}_u$  Average nusselt number  
 $N_{us}$  Nusselt number for smooth channel  
 $N_{ur}$  Nusselt number for rough channel  
 $N_{uav}$  area-averaged Nusselt number  
 $N_{uo}$  Nusselt number for fully developed flow smoothChannel  
 $p/e$  relative roughness pitch  
 $Pr$  Prandtl number  
 $R$  roughness function  
 $Re$  Reynolds number  
 $S_t$  Stanton number  
 $\bar{S}_t$  average Stanton number  
 $S/e$  relative short way length of mesh  
 $W/H$  duct aspect ratio

### Greek symbols

$\phi$  rib chamfer/wedge angle, degree  
 $\eta_{th}$  thermal efficiency  
 $\eta_{eff}$  effective thermal efficiency  
 $\mu$  dynamic viscosity,  $Ns/m^2$   
 $\rho$  density of air,  $kg/m^3$   
 $\alpha$  angle of attack, degree

**References**

- [1] Prasad BN, Saini JS. Effect of artificial roughness on heat transfer and friction factor in a solar air heater. *Solar Energy* 1988;41:555–60.
- [2] Joule JP. On the surface condensation of steam. *Philos Trans R Soc Lond* 1861; 151:133–60.
- [3] Wright LM, Fu WL, Han JC. Thermal performance of angled, V-shaped and Wshaped rib turbulators in rotating rectangular cooling channels (AR = 4:1). *Trans ASME* 2004;126:604–14.
- [4] Han JC, Zhang YM, Lee CP. Augmented heat transfer in square channels with parallel, crossed and v-shaped angled ribs. *Trans ASME J Heat Transfer* 1991; 113:590–6.
- [5] Kays WM, London AL. *Compact heat exchangers*. New York: McGraw Hill; 1966.
- [6] Prasad K, Mullick SC. Heat transfer characteristics of a solar air heater used for drying purposes. *Appl Energy* 1983; 13:83–93.(56)
- [7] Prasad BN, Saini JS. Effect of artificial roughness on heat transfer and friction factor in a solar air heater. *Solar Energy* 1988;41:555–60.(41)
- [8] Prasad BN, Saini JS. Optimal thermohydraulic performance of artificially roughened solar air heaters. *Solar Energy* 1991;47:91–6.(40)
- [9] Verma SK, Prasad BN. Investigation for the optimal thermohydraulic performance of artificially roughened solar air heaters. *Renew Energy* 2000;20:19–36.
- [10] Sahu MM, Bhagoria JL. Augmentation of heat transfer coefficient by using 90 broken transverse ribs on absorber plate of solar air heater. *Renew Energy* 2005;30:2057–63.
- [11] Gupta D, Solanki SC, Saini JS. Thermohydraulic performance of solar air heaters with roughened absorber plates. *Solar Energy* 1997;61:33–42.
- [12] Aharwal KR, Gandhi BK, Saini JS. Experimental investigation on heat-transfer enhancement due to a gap in an inclined continuous rib arrangement in a rectangular duct of solar air heater. *Renew Energy* 2008;33:585–96.
- [13] Momin AME, Saini JS, Solanki SC. Heat transfer and friction in solar air heater duct with v-shaped rib roughness on absorber plate. *Int J Heat Mass Transfer* 2002;45:3383–96.
- [14] Muluwork KB. Investigations on fluid flow and heat transfer in roughened absorber solar heaters. Ph.D. Dissertation 2000; IIT, Roorkee-247667, India.
- [15] Sukhmeet Singh, Subhash Chander, J.S. Saini. Heat transfer and friction factor correlations of solar air heater ducts artificially roughened with discrete V-down ribs. 2011; *Energy* 36 (2011) 5053-5064.
- [16] Hans VS, Saini RP, Saini JS. Heat transfer and friction factor correlations for a solar air heater duct roughened artificially with multiple v-ribs. *Solar Energy* 2010; 84:898-911.
- [17] Karwa RK. Experimental studies of augmented heat transfer and friction in asymmetrically heated rectangular ducts with ribs on heated wall in transverse, inclined, v-continuous and v-discrete pattern. *Int Commun Heat Mass Transfer* 2003;30:241–50.
- [18] Pongjet Promvong. Heat transfer and pressure drop in a channel with multiple 60°V-baffles; *Internationa Communications in Heat and Mass Transfer* 37 (2010) 835–840
- [19] Saini SK, Saini RP. Development of correlations for Nusselt number and friction factor for solar air heater with roughened duct having arc-shaped wire as artificial roughness. *Solar Energy* 2008;82:1118–30.
- [20] Karmare SV, Tikekar AN. Heat transfer and friction factor correlation for artificially roughened duct with metal grit ribs. *Int J Heat Mass Transfer* 2007;50:4342–51.
- [21] Kumar ST, Mittal V, Thakur NS, Kumar A. Heat transfer and friction factor correlations for rectangular solar air heater duct having 60\_ inclined continuous discrete rib arrangement. *Br J Appl Sci Technol* 2011; 3:67-93
- [22] Lau SC, McMillin RD, Han JC. Turbulent heat transfer and friction in a square channel with discrete rib turbulators. *Trans ASME J Turbo Machi* 1991; 113:360-6.
- [23] Karwa R, Solanki SC, Saini JS. Heat transfer coefficient and friction factor correlations for the transitional flow regime in rib-roughened rectangular ducts. *Int J Heat Mass Transfer* 1999;42:1597–615.

- [24] Bhagoria JL, Saini JS, Solanki SC. Heat transfer coefficient and friction factor correlations for rectangular solar air heater duct having transverse wedge shaped rib roughness on the absorber plate. *Renew Energy* 2002;25:341–69.
- [25] Jaurker AR, Saini JS, Gandhi BK. Heat transfer and friction characteristics of rectangular solar air heater duct using rib-grooved artificial roughness. *Solar Energy* 2006;80:895–7.
- [26] Varun, Saini RP, Singal SK. Investigation of thermal performance of solar air heater having roughness elements as a combination of inclined and transverse ribs on absorber plate. *Renew Energy* 2008;133:1398–405.
- [27] Saini RP, Saini JS. Heat transfer and friction factor correlations for artificially roughened ducts with expended metal mesh as roughness element. *Int J Heat Mass Transf* 1997; 40(4):973–86.
- [28] Saini RP, Verma J. Heat transfer and friction factor correlations for a duct having dimple-shaped artificial roughness for solar air heaters. *Energy* 2008;133:1277–87.
- [29] Lau SC, McMillin RD, Han JC. Turbulent heat transfer and friction in a square channel with discrete rib turbulators. *Trans ASME J Turbo Mach* 1991; 113:360-6.